

A. R. Yadao

EXPERIMENTAL VERIFICATION OF EFFECT OF DIFFERENT FLUID PROPERTIES ON THE VIBRATION RESPONSE OF A CANTILEVER ROTOR

Department of Mechanical Engineering G. H. Raisoni College of Engineering and Management Pune Indi; email: adik.mech@gmail.com

Abstract. The current analysis is an effort to obtain the vibration characteristics of the cantilever rotor shaft with an extra mass added at the free end of the rotor shaft partially immersed in the viscous medium. This work is concentrated on the theoretical analysis of the natural frequency and amplitude of the spinning cantilever rotor shaft with addition mass using the influence coefficient method. The influence of fluid forces is studied using the Navier-Stoke's equation. The gap ratio (ratio of the fluid-filled container radius to the shaft radius) and viscosity of the fluid are taken as the main variable parameters. MATLAB programming is used to obtaining vibration behavior from the theoretical expressions. An obtained result from the numerical analysis is validated by the comparison of the results of experimental analysis.

Keywords: cantilever rotor shaft, dynamic response, Navier-Stoke's equation, influence coefficient method.

1. Introduction.

In the last few years, the researchers focused on the dynamic analysis of the critical speed of the rotor, under several conditions, due to its significance in design. When a shaft rotates in a viscous medium, the analysis of natural frequency and amplitudes becomes difficult. The effects of a crack in the shaft of rotating machinery associated with dynamic analysis were determined by many investigators. The researchers are done a lot of work on the vibration response of the shaft. But no particular analysis of the rotor shaft in a different fluid medium is described. The current analysis is helpful for the vibration characteristics of the rotating shaft in a viscous fluid such as high-speed turbine rotors, long spinning shaft used for the extracting oil from the seabed by drilling, etc.

Wauer [1] has reported a review of the dynamics of a cracked rotor. Kedyrow et al. [2] have studied the vibration analysis of the oscillation of cylinder immersed inside the viscous fluid-filled tubular duct. They have used theoretical and mathematical significance for obtained the frequency with consideration of different fluid parameter Walston et al. [3] have investigated the vibration characteristics of a spinning shaft inside a viscous medium, but no exact distinction was made among the damping effect and virtual mass effect on the spinning shaft. Papadopoulos and Dimarogonas [4] have discussed the dynamic characteristics of a spinning shaft with transverse crack, but they have not discussed the separately external damping effect and virtual mass effect on the crack shaft. Ostachowicz and Krawczuk [5] have studied the effect of transverse cracks on coupled torsional and bending vibrations of a rotor. Gasch [6] has studied the dynamic response of a spinning shaft with a transverse crack. They took the De-Laval rotor for the investigation and explored some prospects for early crack identification. Fritz [7] has examined a spinning rod in a cylindrical vessel with consideration of the effect of Taylor vortex and turbulence for a small rod cylinder gap. Cho-Chung et al. [8] have investigated a simple technique to define the vibration mode shapes and frequencies of cantilever plates which are submerged in the fluid medium based on empirical added mass formulation. Sol [9] has analyzed the dynamic behavior of the

cracked shaft with critical speed. They have obtained analytical results compare with the results of experimental analysis. Brenner [10] has investigated the theoretically the fluid forces acting on spinning rod inside the circular cylinder for low and high Reynolds numbers. Walston et al. [11] have reported the vibration analysis of a rotating shaft submerged inside the viscous fluid. The effect of the fluid forces on the dynamic response of the rotor evaluate experimentally and by using the statistical regression analysis, obtained the equation of amplitude as a function of viscosity, velocity and mass. Achenbach et al. [12] have presented the vibration analysis of an immersed beam of circular cross-section using mathematical methods. Han and Chu [13] have studied the dynamic instability of the breathing cracked rotating shaft. Xiaohui et al. [14] based on the Rayleigh-Ritz formulation and green function method, presented the dynamic analysis of the cracked rectangular plate with the infinite water field. Awlad et al. [15] have investigated numerically the dynamic characteristics of cantilever beam which is partially submerged inside the viscous fluid. Also they have done the experimental verification by using polytech scanning vibrometer.

Hahgholi et al. [16] have studied the dynamic analysis of a nonlinear rotating simply support shaft. In the modeling of the system rotary inertia and gyroscopic effect are considered. The equations of motion are derived with the help of the extended Hamilton principle. Catherine et al. [17] have investigated the vibrations characteristics of a cantilever beam of rectangular cross section immersed in a viscous fluid under harmonic base excitation. The Interactions between fluid and structure are demonstrated by a complex hydrodynamic function which is defines additional mass and damping effect in dynamic response of large alteration of amplitudes.

In this article, a systematic investigation for the vibration characteristics of a spinning cantilever rotor shaft in viscous fluid medium is presented. The external fluid force is calculated with the help of Navier Stoke's equation. Dynamic response (i.e. Natural frequency, amplitude)of the rotor shaft is obtained using the influence coefficients method. Finally, the numerical analysis results are compared with the developed experimental analysis results.

2. Theoretical analysis.

2.1 Equation of motion. Figure1 represents a fixed-fixed type rotating shaft in which the X-Y coordinate system and the point 'O' indicate the center of spinning shaft. The point 'ó' rotating around the point 'O' with whirling speed ' Ω ' and whirling radius ' δ '.

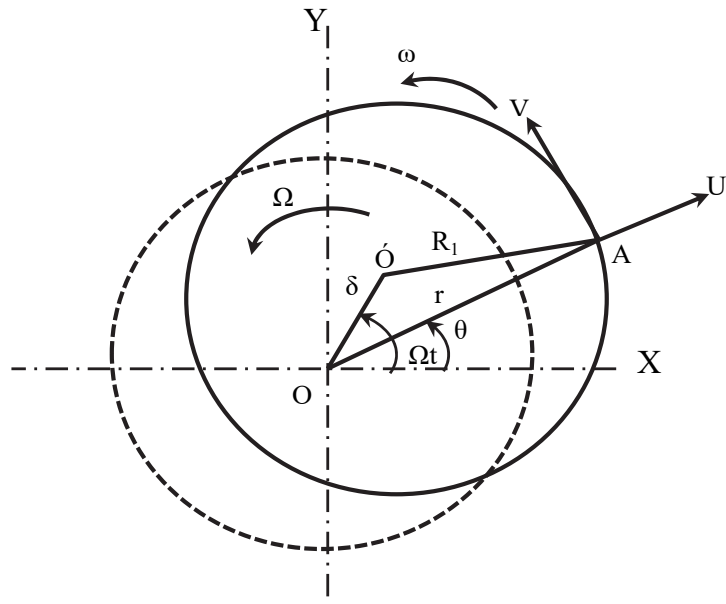


Fig. 1. Whirling speed of the rotor shaft

In polar coordinates of the Navier Stroke's equation can be expressed as,

$$\frac{1}{\rho} \frac{\partial p}{\partial r} - \nu \left(\frac{\partial^2 u}{\partial r^2} + \frac{1}{r} \frac{\partial u}{\partial r} - \frac{2}{r^2} \frac{\partial v}{\partial \theta} - \frac{u}{r^2} + \frac{1}{r^2} \frac{\partial^2 u}{\partial \theta^2} \right) + \frac{\partial u}{\partial t} = 0; \quad (1a)$$

$$\frac{1}{\rho r} \frac{\partial p}{\partial \theta} - \nu \left(\frac{\partial^2 v}{\partial r^2} + \frac{1}{r} \frac{\partial v}{\partial r} + \frac{2}{r^2} \frac{\partial u}{\partial \theta} - \frac{v}{r^2} + \frac{1}{r^2} \frac{\partial^2 v}{\partial \theta^2} \right) + \frac{\partial v}{\partial t} = 0. \quad (1b)$$

According to the non-stationary components of radial and tangential velocities of the rotor shaft are given as follows:

$$u_{nc} = -\frac{1}{r} \frac{\partial \phi}{\partial \theta} = j\delta\omega \left[A \left(\frac{R_1}{r} \right)^2 + B + C \left(\frac{R_1}{r} \right) I_1(kr) + D \left(\frac{R_1}{r} \right) K_1(kr) \right] e^{j(\omega t - \theta)}; \quad (2a)$$

$$v_{nc} = \frac{\partial \phi}{\partial r} = \\ = \delta\omega \left[-A \left(\frac{R_1}{r} \right)^2 + B + C \left\{ -\left(\frac{R_1}{r} \right) I_1(kr) + kR_1 I_0(kr) \right\} + D \left\{ -\left(\frac{R_1}{r} \right) K_1(kr) - kR_1 K_0(kr) \right\} \right] e^{j(\omega t - \theta)}. \quad (2b)$$

2.2 Analysis of fluid forces. Substituting the velocities of external fluid flow into the equation (1), the pressure (P) can be calculated as

$$P = \int \frac{dp}{dq} dq = dr w^2 \left\{ \frac{-A}{r} R_1^2 + Br \right\} e^{j(\omega t - q)} \frac{dy}{dx}. \quad (3)$$

The direct stress (τ_r) and circumferential stress ($\tau_{r\theta}$) can be expressed as,

$$2m \frac{du_i}{dr} - p = t_{rr} \text{ and } m \left(r \frac{d}{dr} \left(\frac{n_i}{r} \right) + \frac{1}{r} \frac{du_i}{dq} \right) = t_{r\theta}. \quad (4)$$

External fluid force impact on the rotor shaft at the both directions (i.e. x and y) are determined as

$$F_x = \int_0^{2\pi} (\tau_{rr} \cos \theta - \tau_{r\theta} \sin \theta) R_1 d\theta = m\delta\omega^2 \{A - B - CI_1(\alpha) - DK_1(\alpha)\} e^{j\omega t}; \quad (5a)$$

$$F_y = \int_0^{2\pi} (\tau_{rr} \sin \theta + \tau_{r\theta} \cos \theta) R_1 d\theta = -im\delta\omega^2 \{A - B - CI_1(\alpha) - DK_1(\alpha)\} e^{j\omega t}. \quad (5b)$$

2.3 Equation of rotor motion. In the current study, the cantilever rotor shaft with a disc at the mid-span of the shaft which is immersed inside the fluid medium has been considered. Firstly, here consider the equivalent lump mass of rotor shaft is determined. After that the additional masses is added and calculate the overall lumped mass of the rotor system.

The equivalent lump, mass of the system can be expressed:

$$\alpha_{eq1} = \frac{K_{44}}{\omega_{44}^2 M_{s2}} \text{ and } a_{eq2} = \frac{K_{55}}{\omega_{55}^2 M_{s2}}.$$

The whole mass of the cantilever rotor shaft becomes

$$M_{s1} + \alpha_{eq1} M_{s2} - M_1 M_s = 0 \text{ and } M_{s1} + \alpha_{eq2} M_{s2} - M_2 M_s = 0;$$

$$F_x = K_{44}X + M_1 M_s \frac{d^2(X + \varepsilon \cos \omega t)}{dt^2}; \quad (6a)$$

$$F_y = K_{55}Y + \frac{d^2(Y + \varepsilon \sin \omega t)}{dt^2} M_2 M_s. \quad (6b)$$

The equation (6) can be rewritten as,

$$F_x = M\omega \operatorname{Im}(H) \frac{dx}{dt} - M \operatorname{Re}(H) \frac{d^2x}{dt^2}; \quad (7a)$$

$$F_y = M\omega \operatorname{Im}(H) \frac{dy}{dt} - M \operatorname{Re}(H) \frac{d^2y}{dt^2}. \quad (7b)$$

Where $M_1 \operatorname{Re}(H_1) + M_2 \alpha_{eq} \operatorname{Re}(H_2) = M \operatorname{Re}(H)$

$$M_1 \operatorname{Im}(H_1) + M_2 \alpha_{eq} \operatorname{Re}(H_2) = M \operatorname{Im}(H);$$

$$M_1 + M_2 \alpha_{eq} = M.$$

Where M_1 = Fluid mass moved by the additional mass and M_2 = fluid mass moved by rotor shaft.

$$K_s x + (M \operatorname{Re}(H) + M_s) \frac{d^2x}{dt^2} - M\omega \operatorname{Im}(H) \frac{dx}{dt} - M_s \varepsilon \omega^2 \cos \omega t = 0; \quad (8a)$$

$$K_s y + (M \operatorname{Re}(H) + M_s) \frac{d^2y}{dt^2} - M\omega \operatorname{Im}(H) \frac{dy}{dt} - M_s \varepsilon \omega^2 \sin \omega t = 0. \quad (8b)$$

Taking the eccentricity ε_1 and ε_2 . Primarily, ε_1 is considered for X- axis Dirⁿ and Y-axis Dirⁿ is finding out in the subsequent method.

$$(1 + M_1^* \operatorname{Re}(H)) \frac{d^2\xi_2}{dt_1^2} - M_1^* \omega_1^* \operatorname{Im}(H) \frac{d\xi_2}{d\tau_1} + \xi_2 = \varepsilon_1^* (\omega_1^*)^2 \cos(\omega_1^* \tau_1); \quad (9a)$$

$$(1 + M_2^* \operatorname{Re}(H)) \frac{d^2\eta_2}{dt_2^2} - M_2^* \omega_2^* \operatorname{Im}(H) \frac{d\eta_2}{d\tau_2} + \eta_2 = \varepsilon_2^* (\omega_2^*)^2 \sin(\omega_2^* \tau_2). \quad (9b)$$

By solving equation (9), we can get a the non-dimensional form as

$$\frac{A}{\sqrt{(C\omega^2)^2 + (K - (\omega^*)^2)^2}} = \delta^*; \quad \phi = \tan^{-1} \left(\frac{C\omega^*}{K - (\omega^*)^2} \right);$$

$$C = \frac{-m^* \omega^* \operatorname{Im}(H)}{1 + m^* \operatorname{Re}(H)}; \quad \frac{\varepsilon^* (\omega^*)^2}{M^* \operatorname{Re}(H) + 1} = A.$$

Where δ^* is the maximum non-dimensional amplitude

3. Numerical analysis and discussions.

Different parameters of the cantilever rotor shaft for numerical and experimental analysis are given below in Table 1.

Table 1. Parameters related to vibration behavior of cantilever rotor shaft.

S.N.	Parameters	Value (Unit)	
01	Material of rotor shaft	Mild steel	
02	Density of shaft material	$\rho = 7850 \text{ kg/m}^3$	
03	Radius of the rotor shaft	$R_1 = 0,01\text{m}$	
04	Length of rotor shaft	$L = 0,8\text{m}$	
05	Gap ratio(R_2-R_1/R_1)	$q = 6, 12, 16, 20$	
06	Mass of disc	$M_{Disc} = 0,55\text{kg}$	
07	Radius of the disc	$R_D = 0,035\text{m}$	
08	Thickness of disc	$T_D = 0,022\text{m}$	
09	Three different type of viscous fluid		
10	Fluid Name	Kinematic viscosity $v(\text{stokes})$	Ratio of density (M^*)
11	Water	0,0633	0,144
12	Palm oil	0,541	0,153
13	Lubricant oil 2T	2,4	0,158

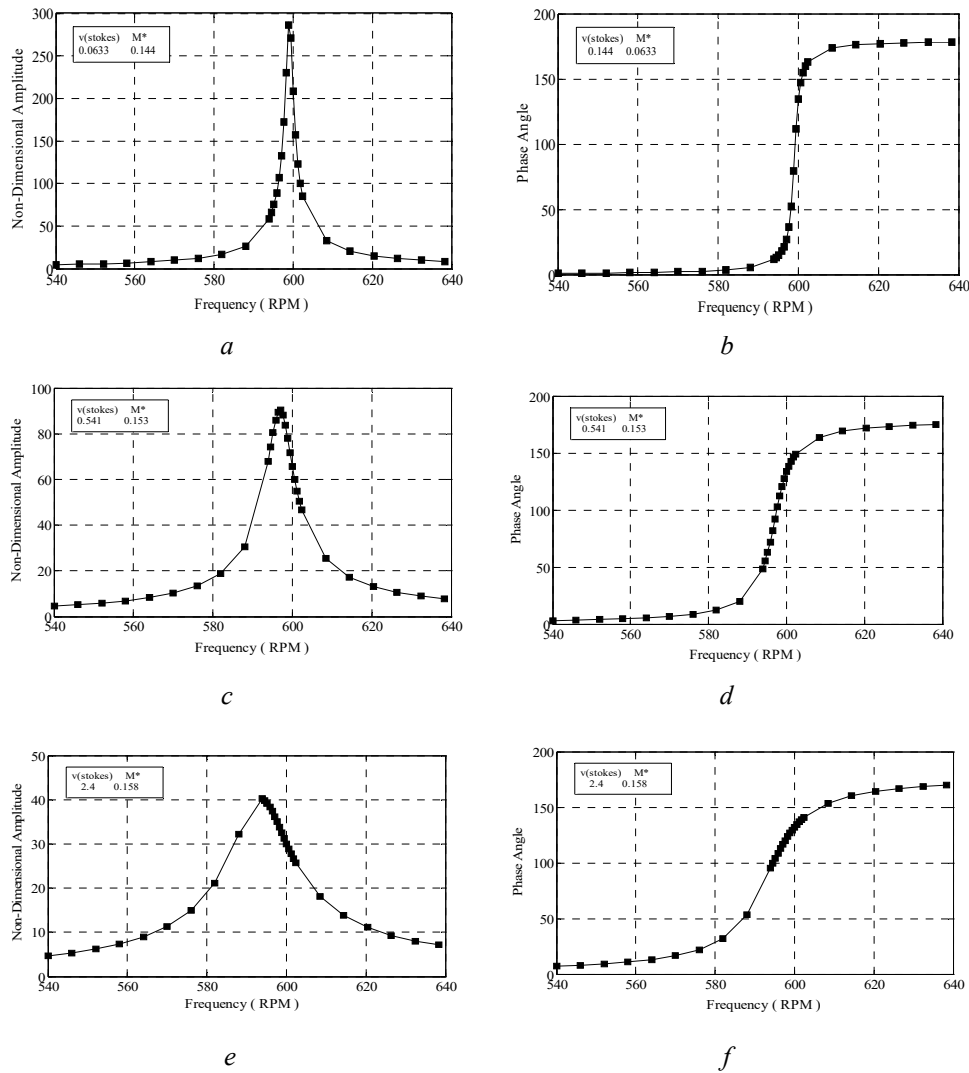


Fig.2. (a, c, e) Frequency (ω) Vs Non-Dimensional amplitude (δ_n^*/ϵ^*),
(b, d, f) Frequency (ω) Vs Phase angle (ϕ), Mild Steel Shaft, $R_1= 0,01\text{m}$,
 $L= 0,8\text{m}$, $q=12$, $M_D= 0,55\text{kg}$, $T_D= 0,022\text{m}$

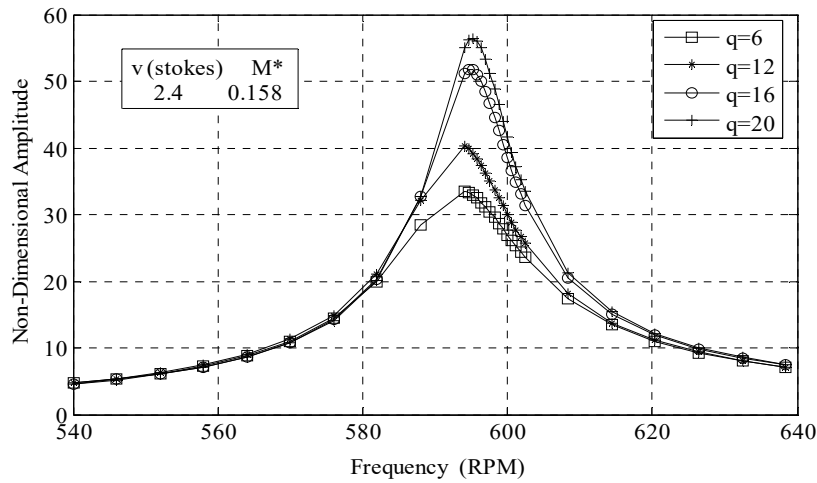


Fig. 3. Frequency (ω) Vs Non-Dimensional amplitude (δ_n^*/ε^*),
Mild Steel Shaft, $R_1=0,01\text{m}$, $L=0,8\text{m}$, $M_D=0,55\text{kg}$, $T_D=0,022\text{m}$

3.1 Discussion. Fig. 2 shows the influence of different viscosity's of viscous fluid on the dynamic response of the cantilever rotor shaft. It is found that as the viscosity of fluid medium increases the whirling speed of the rotor shaft and the amplitude of vibration fall down due to increase in virtual mass. Fig. 3 shows the effect of different gap ratio on the dynamic response of the rotor shaft. It is observed that the amplitude of vibration increases due to increases the radius of the fluid filled container.

4. Experimental analysis.

To compare the obtained results of the theoretical analysis, experimental analyses have been done in a spinning cantilever rotor shaft inside the various fluid medium. For this purpose we have developed an experimental setup which comprises the rotor shaft with extra mass (i.e. disc), variac, power motor, three ultrasonic sensors, microcontroller, bread board, USB connection serial port and response display devices (i.e. Computer system) as shown in Fig. 4.

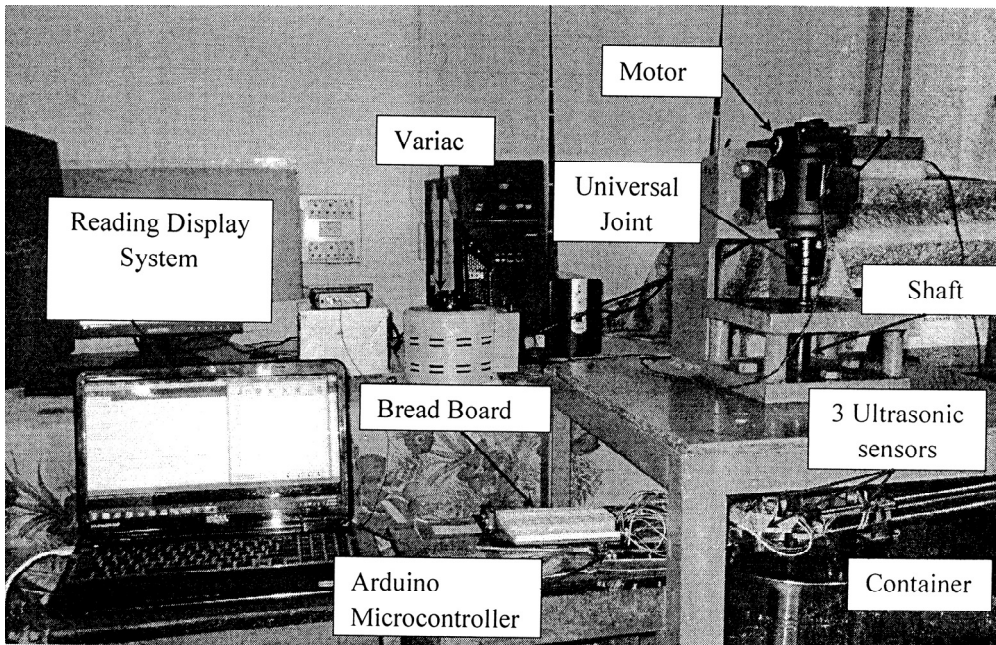


Fig. 4. Experimental Setup of cantilever rotor shaft system with viscous medium.

Experiments have been conducted on the rotating cantilever rotor shaft with attached mass at the free end in the different viscous fluid medium. The inner radius and length of the fluid-filled container are 260 mm and 400 mm respectively. The shaft of the power motor is connected with the rotor shaft with the help of universal joint. Variac is used to control the speed of the spinning rotor shaft. The rotating shaft is supported by ball bearing. In this work the bearing effect is not taken into account in order to simplify for the rotor system. The rotating speed of the rotor shaft is taken in the range of 300 to 700 rpm. The three ultrasonic sensors are arranged around the rotating cantilever rotor shaft in the viscous fluid is connected to the Arduino microcontroller by using the bread board and jumper wire is used to obtain the deflection of the rotor shaft from starting position. Each sensor has separate deflection data of the rotor motion. For accuracy, reading has been taken for three times at the same speed. Each set have 900 samples measured by sensors within 15 minutes (i.e. sampling time 1sec/sample).

Table 2. Detail of parts of experimental test rig of cantilever rotor shaft system.

S.N.	Name of different parts of experimental test rig
1	Mild Steel cantilever rotor shaft Shaft length (L) = 0,8; Radius of shaft (R_1) = 0,01m
2	Radius of liquid filled vessel 13cm
3	Power supply, 50Hz , 230 to 240v AC
4	Taco meter: Telco Hand Taco meters, Type: H 10000 rpm
5	Driving unit (Motor, Type AC/DC, 220 v , 125 watt ,6000 rpm)
6	Variac, Input: 230v, Output: 0 to 270 v, 50 to 60 Hz
7	Bread board
8	USB connection Serial Port
9	Microcontroller, Arduino UNO A Tmega328, Analog Input Pins 6, Digital Input Pins 14, Input voltage 6-20V, Operating Voltage 5V.
10	3 Ultrasonic Sensors,Range of distance measure: 0.01m to 4.5 m Operating Voltage: DC 5V, Operating Current: less than 15mA,Response Time: 100ms

Table 3. Effect of the different viscosity of fluid medium on the amplitude of the rotor shaft.

S.N.	Numerical results		Experimental results				% Error		
	Three different viscosity (η) in Stokes								
	2,4	0,541	0,0633	2,4	0,541	0,0633	2,4	0,541	0,0633
1	4,704	4,445	4,328	4,887	4,582	4,522	3,9	3,1	4,5
2	7,383	6,808	6,546	7,597	7,114	6,801	2,9	4,5	3,9
3	14,896	13,124	12,239	15,673	13,465	12,899	5,2	2,6	5,4
4	40,244	68,160	57,932	41,491	71,022	56,309	3,1	4,2	- 2,8
5	38,359	91,848	88,496	40,123	95,614	92,478	4,6	4,1	4,5
6	33,782	96,964	230,615	34,998	94,443	224,157	3,6	- 2,6	- 2,8
7	30,062	74,084	207,944	31,475	77,492	217,509	3,1	4,6	4,6
8	26,673	55,157	100,519	27,927	57,143	104,439	4,7	3,6	3,9
9	11,112	13,425	14,687	11,489	13,035	14,305	3,4	- 2,9	- 2,6
10	7,122	7,931	8,333	7,421	7,724	8,566	4,2	- 2,6	2,8

Table 4. Effect of different gap ratio on the amplitude of rotor shaft.

S.N.	Numerical results			Experimental results			% Error		
	Three different gap ratio(ratio of vessel radius to shaft radius)								
	q1=12	q2=16	q3=20	q1=12	q2=16	q3=20	q1=12	q2=16	q3=20
1	4,704	7,165	7,117	4,887	7,458	7,302	3,9	4,1	2,6
2	7,383	14,269	14,130	7,597	14,768	14,723	2,9	3,5	4,2
3	14,896	51,735	56,122	15,673	53,907	57,974	5,2	4,2	3,3,
4	40,244	49,944	54,972	41,491	51,742	56,511	3,1	3,6	2,8
5	38,359	44,650	48,916	40,123	45,677	50,334	4,6	2,3	2,9
6	33,782	38,526	41,647	34,998	39,489	42,938	3,6	2,5	3,1
7	30,062	33,052	35,249	31,475	34,241	36,024	3,1	3,6	2,2
8	26,673	15,074	15,429	27,927	15,32	15,953	4,7	1,6	3,4
9	11,112	9,867	10,000	11,489	10,153	10,21	3,4	2,9	2,1
10	7,122	7,413	7,486	7,421	7,826	7,845	4,2	4,6	4,8

Table 3 shows the comparison of the obtained numerical and experimental result of amplitude of shaft due to influence of the different viscosity of the viscous fluid. Table 4 shows the comparison of the obtained numerical and experimental results of amplitude of vibration due to effect of different gap ratio (i.e. ratio of the radius of fluid vessel to the radius of rotor shaft). The result of numerical analysis was compared with the obtained experimental results. It was found to be good agreement.

5. Conclusions.

In the current investigation, presented the dynamic analysis of cantilever rotor shaft immersed in a fluid medium was firstly obtained by the numerical analysis which determined by the MATLAB programming. Then the result of the numerical analysis was compared with the results of developed experimental analysis of test rig. It is found to be very good agreement. The viscosity and density of the viscous fluid in which spinning cantilever rotor shaft was immersed were observed to remarkable effect on its vibration characteristics. The fundamental natural frequency of the rotor shaft and amplitude of vibration was observed to be fall down with the increased fluid viscosity and density. The phase lag of the rotor shaft is varied due to the existence of viscous fluid. An amplitude of vibration is increased while increases the gap ratio of the cantilever rotor system.

Nomenclature	
A = Cross-sectional area of rotor D = Diameter of rotor shaft E = Young's modulus of elasticity h = Height of rectangular strip i = Variable I = Moment of inertia Ks = Stiffness of the shaft L = Length of shaft m = Fluid mass displaced by the shaft per unit length m _s = Rotor shaft mass per unit length M* = Dimensionless parameter (m/m _s)	M _D = Mass of disc q = Gap ratio (R ₂ -R ₁ /R ₁) R _D = Radius of disc R ₁ = Radius of the rotor shaft R ₂ = Radius of the fluid vessel T _D = Thickness of disc u = Radial flow velocity v = Tangential flow velocity ϵ^* = ϵ_1/R_1 ϵ = Eccentricity of mass of disc from its geometry center Ω = Angular velocity of whirling

РЕЗЮМЕ. Запропонований аналіз має метою отримати характеристики коливань валу консольного ротора з додатковою масою на вільному кінці валу, частково зануреного у в'язке середовище. Ця робота зосереджена на теоретичному аналізі власних частот та амплітуд обертового консольного валу з додатковою масою з використанням методу коефіцієнта впливу. Вплив сил рідини вивчається за допомогою рівняння Нав'є-Стокса. Коефіцієнт зазору (відношення радіуса ємності, наповненої рідиною, до радіуса валу) та в'язкість рідини приймаються за основні змінні параметри. Для отримання вібраційної поведінки з теоретичних виразів використовується програмування MATLAB. Отриманий результат чисельного аналізу підтверджується порівнянням з результатами експериментального аналізу.

1. Wauer J. On the dynamics of cracked rotors: A literature survey // Appl. Mech. Review. – 1990. – **43**, N 1. – P. 13 – 17.
2. Kadyrov S.G., Wauer J., Sorokin S.V. A potential technique in the theory of interaction between a structure and a viscous, compressible fluid // Archive of Appl. Mech. – 2001. – **71**. – P. 405 – 417.
3. Walston W.H., Ames W.F., Clark L.G. Dynamic stability of rotating shafts in viscous fluids // ASME J. of Appl. Mech. – 1964. – **31**, N 2. – P. 292 – 299.
4. Papadopoulos C.A., Dimarogonas A.D. Coupled longitudinal and bending vibrations of a rotating shaft with an open crack // J. of Sound and Vibration. – 1987. – **117**, N 1. – P. 81 – 93.
5. Ostachowicz W.M., Krawczuk M. Coupled torsional and bending vibrations of a rotor with an open crack // Archive of Appl. Mech. – 1996. – **62**, N 3. – P. 191 – 201.
6. Gasch R. A survey of the dynamic behaviour of a simple rotating shaft with a transverse crack // J. of Sound and Vibration. – 1993. – **160**, N 2. – P. 313 – 332.
7. Fritz R.J. The effects of an annular fluid on the vibrations of a long rotor. Part 1: Theory // J. of Basic Engineering. – 1970. – **92**, N 4. – P. 923 – 930.
8. Cho-Chung L., Ching-Chao L., Yuh-Shiou T., Wen-Hao L. The free vibration analysis of submerged cantilever plates // Ocean Engineering. – 2001. – **28**, N 9. – P. 1225 – 1245.
9. Sol J.C. Vibration detection of a transverse crack in a rotating machine shaft // Mecanique Materiaux Electricite. – 1980. – **371**. – P. 404 – 409.
10. Brennen C. On the flow in an annulus surrounding a whirling cylinder // J. of Fluid Mech. – 1976. – **75**, N 1. – P. 173 – 191.
11. Walston W.H., Ames W.F., Clark L.G. Dynamic stability of rotating shafts in viscous fluids // ASME, J. of Appl. Mech. – 1964. – **31**, N 2. – P. 292 – 299.
12. Achenbach J.D., Qu J. Resonant vibrations of a submerged // J. of Sound and Vibration. – 1986. – **105**, N 2. – P. 185 – 198.
13. Han Q., Chu F. Dynamic instability and steady-state response of an elliptical cracked shaft // Arch. Appl. Mech. – 2012. – **82**. – P. 709 – 722.
14. Xiaohui S., Wenxiu L., Fulei C. Dynamic analysis of rectangular plates with a single side crack and in contact with water on one side based on the Rayleigh–Ritz method // J. of Fluids and Structures. – 2012. – **34**. – P. 90 – 104.
15. Hossain A., Humphrey L., Mian A. Prediction of the dynamic response of a mini-cantilever beam partially submerged in viscous media using finite element method // Finite Element Anal. Des. – 2012. – **48**. – P. 1339 – 1345.
16. Shahgholi M., Khadem S.E., Bab S. Free vibration analysis of a nonlinear slender rotating shaft with simply support conditions // Mechanism and Machine Theory. – 2014. – **82**. – P. 128 – 140.
17. Catherine N.P., Matteo A.I., Maurizio P. Finite amplitude vibrations of cantilevers of rectangular cross sections in viscous fluids // J. of Fluids and Structures. – 2013. – **40**. – P. 52 – 69.

*From the Editorial Board: The article corresponds completely to submitted manuscript.